Biosci. Rep. (2012) / **32** / 631–639 (Printed in Great Britain) / doi 10.1042/BSR20120046

Protein instability and functional defects caused by mutations of dihydro-orotate dehydrogenase in Miller syndrome patients

JingXian FANG*†, Takeshi UCHIUMI*[1], Mikako YAGI*, Shinya MATSUMOTO*, Rie AMAMOTO*, Toshiro SAITO*, Shinya TAKAZAKI*, Tomotake KANKI*, Haruyoshi YAMAZA†, Kazuaki NONAKA† and Dongchon KANG*

*Department of Clinical Chemistry and Laboratory Medicine, Graduate School of Medical Sciences, Kyushu University, 3-1-1 Maidashi, Higashi-ku, Fukuoka 812-8582, Japan, and †Department of Pediatric Dentistry, Graduate School of Dental Science, Kyushu University, 3-1-1 Maidashi, Higashi-ku, Fukuoka 812-8582, Japan

Synopsis

Miller syndrome is a recessive inherited disorder characterized by postaxial acrofacial dysostosis. It is caused by dysfunction of the *DHODH* (dihydroorotate dehydrogenase) gene, which encodes a key enzyme in the pyrimidine *de novo* biosynthesis pathway and is localized at mitochondria intermembrane space. We investigated the consequence of three missense mutations, G202A, R346W and R135C of DHODH, which were previously identified in patients with Miller syndrome. First, we established HeLa cell lines stably expressing DHODH with Miller syndrome-causative mutations: G202A, R346W and R135C. These three mutant proteins retained the proper mitochondrial localization based on immunohistochemistry and mitochondrial subfractionation studies. The G202A, R346W DHODH proteins showed reduced protein stability. On the other hand, the third one R135C, in which the mutation lies at the ubiquinone-binding site, was stable but possessed no enzymatic activity. In conclusion, the G202A and R346W mutation causes deficient protein stability, and the R135C mutation does not affect stability but impairs the substrate-induced enzymatic activity, suggesting that impairment of DHODH activity is linked to the Miller syndrome phenotype.

Key words: dihydro-orotate dehydrogenase (DHODH), Miller syndrome, missense mutation, mitochondrion, protein stability

INTRODUCTION

The mitochondrion is a double membrane-enclosed organelle that is regarded as the energy factory of eukaryotic cells because of its energy conversion function. However, mitochondria also participate in calcium and iron storage as well as having important functions in signalling, cell differentiation, cell death, and the control of cell cycle and cell growth [1]. Recent studies have shown that mitochondrial dysfunction is responsible for a wide range of human diseases, and mitochondria have a possible relationship with aging [2,3]. Given that the majority of ATP production depends on the respiratory chain, maintenance of the mitochondrial genome is critical for individuals to maintain normal health [4,5].

Pyrimidine nucleotides are synthesized through two pathways: the *de novo* synthesis pathway and the salvage pathway. The enzyme DHODH (dihydro-orotate dehydrogenase) catalyses the fourth step in the *de novo* biosynthesis of pyrimidine by converting DHO (dihydro-orotate) into orotate [6,7]. DHODH is also the only enzyme of this pyrimidine biosynthesis pathway that is located on the inner membrane of mitochondria, while all the other enzymes are located within the cytosol. DHODH catalyses the oxidation of DHO to orotate by transferring electrons to the respiratory molecule ubiquinone through an enzyme-bound redox cofactor flavin mononucleotide [8]. Thus, DHODH relies on ubiquinone, thereby forming a functional link between the mitochondrial respiratory chain and pyrimidine biosynthesis.

DHODH has two binding sites. The substrate DHO binds to the first site and is oxidized *via* a co-substrate electron acceptor. After the release of orotate, ubiquinone binds to a second site and receives an electron from the co-substrate. The orotate synthesized by DHODH is converted into UMP (uridine monophosphate) by the enzyme complex UMPS (UMP synthase) [9,10].

Abbreviations used: anti-HA, anti-haemagglutinin; CHX, cycloheximide; DCPIP, dichlorophenolindophenol; DHFR, dihydrofolate reductase; DHO, dihydroorotate; DHODH, dihydro-orotate dehydrogenase; DHODH-HA, DHODH with a C-terminal HA tag; DMEM, Dulbecco's modified Eagle's medium; DOX, doxycycline; FBS, fetal bovine serum; LFN, leflunomide; OXPHOS, oxidative phosphorylation; TFAM, mitochondrial transcription factor A; UMPS, UMP synthase.

[1] To whom correspondence should be addressed (email uchiumi@cclm.med.kyushu-u.ac.jp).

Miller syndrome is a type of acrofacial dysostosis, also known as Wildervanck–Smith syndrome. Its clinical features consist of severe micrognathia, cleft lip and/or palate, hypoplasia or aplasia of the postaxial elements of the limbs, coloboma of the eyelids and supernumerary nipples [11,12]. The mutant gene responsible for the disorder has been found recently to be *DHODH*, which is located at chromosome 16q22 [13]. A total of 13 mutations in the *DHODH* gene have been reported in Miller syndrome, from exon 2 to exon 9 [13,14]. However, it is unknown how mutations in *DHODH* cause the phenotype of Miller syndrome.

In mice, use of the DHODH inhibitor LFN (leflunomide) during pregnancy causes a wide range of limb and craniofacial defects, the most common of which are exencephaly, cleft palate and failure of the eyelid to close [15]. Thus, the evidence that *DHODH* mutations cause Miller syndrome reveals a new role for DHODH in craniofacial and limb development that remains to be explored. In the present study, we investigated the effects of three Miller syndrome-associated DHODH mutations on protein stability, localization and the DHO-dependent enzymatic activity of DHODH in mitochondria. We observed that DHODH plays an important role in Miller syndrome.

EXPERIMENTAL

Antibodies and chemicals

Anti-DHODH, anti-HA (anti-haemagglutinin) and anti-TFAM (mitochondrial transcription factor A) antibodies were raised in our own laboratory. Anti-BAP37 was purchased from Santa Cruz Biotechnology. Anti-β-actin was purchased from Sigma. MitoTracker Red was purchased from Invitrogen. L-DHO was purchased from Sigma.

Cell culture

Human cervical cancer HeLa cells were cultured in DMEM (Dulbecco's modified Eagle's medium) (Sigma) with 10% heat-inactivated FBS (fetal bovine serum). Cell lines were maintained in a 5% CO_2 atmosphere at 37 °C.

Expression constructs

An expression construct containing the *DHODH* cDNA was generated by standard methods. cDNAs of wild-type and mutant *DHODH* were cloned into the BamHI/XhoI sites of the expression vector pcDNA5 (Invitrogen). A *DHODH* cDNA containing the deduced first methionine site was amplified from a cDNA library of human HeLa cells by PCR using the following primer set: 5′-CAGAGTCTTCTGCCTCCCTG-3′ and 5′-CAGGGAGGCAGAAGACTCTG-3′. Then, BamHI and XhoI sites were added to the 5′- and 3′-terminals respectively of the cDNA by a second PCR using the primers 5′-GGATCCATGGCGTGGAGACACCTGAAAAAGC-3′ and 5′-CTCGAGTCACCTCCGATGATCTGCTCC-3′. The PCR product was digested with BamHI and XhoI. The DNA fragment encoding DHODH, a DNA fragment encoding an HA-tag and a pcDNA5/FRT vector (Invitrogen) were digested with BamHI and XhoI and ligated together. The vector was named pDHODH-HA.

Construction of mutant DHODH expression plasmids

The DHODH mutants G202A, R346W and R135C were generated from pDHODH-HA. The mutants were generated by PCR-based site-directed mutagenesis [16]. All PCR-generated fragments were confirmed by sequencing after insertion into the pGEM-T vector (Promega), and expression vectors were constructed with pcDNA5/FRT (Invitrogen).

To generate stable inducible cell lines, HeLa Flp-In™ T-Rex™ cells (Invitrogen) were co-transfected with pcDNA5/FRT/TO harbouring *DHODH* and pOG44 using Lipofectamine™ 2000 (Invitrogen) transfection reagent according to the manufacturer's instructions. After transfection, cells were cultured in DMEM containing hygromycin B (200 μg/ml) and blasticidin S (10 μg/ml) (Invitrogen). After selection for approximately 3–4 weeks, clonal foci were identified, transferred into separate wells, and checked for expression using the anti-HA antibody. Expression was induced by the addition of DOX (doxycycline; 1 μg/ml) to the culture medium for the indicated time.

Immunoblotting

HeLa cells were lysed in TNE lysis buffer (50 mM Tris/HCl, pH 7.5, 1 mM EDTA, 150 mM NaCl and 0.5% Nonidet P40) and proteins (20 μg) were separated by SDS/PAGE and immunoblotted with the indicated specific antibodies. The signals were visualized with horseradish-peroxidase-labelled anti-rabbit IgG and an enhanced chemiluminescence reagent (GE Healthcare). The chemiluminescence was recorded and quantified with a chilled charge-coupled device camera (LAS1000plus; Fuji Photo Film).

Submitochondrial localization

HeLa cells (10^8 cells) were scraped off with a cell lifter, suspended in PBS, precipitated by centrifugation, and washed with homogenizing buffer. The supernatant was centrifuged at 10000 ***g*** for 6 min. The pellet was collected as a crude mitochondrial fraction. The crude mitochondria (20 μg) were suspended in hypotonic buffer (10 mM Hepes/KOH, pH 7.4 and 1 mM EDTA) at 4 °C to disrupt the mitochondrial outer membrane. After the hypotonic treatment, the mitochondria were precipitated by centrifugation at 10000 ***g*** for 6 min. The mitochondria were resuspended in hypotonic buffer and then digested with proteinase K (200 μg/ml) with or without 1% Triton X-100 on ice for 20 min. The protein was precipitated by the addition of 15% trichloroacetic acid. The precipitates were solubilized in sample buffer (6% SDS, 150 mM Tris base, 10 mM EDTA and 25% glycerol), separated by SDS/PAGE and analysed by immunoblotting.

Immunofluorescent imaging of HeLa cells

Immunofluorescence was carried out according to established techniques. Briefly, HeLa cells were incubated in the presence of 500 nM MitoTracker Red (Invitrogen) for 20 min. Cells were fixed and permeabilized, then incubated with a 1:200 dilution of anti-HA and anti-DHODH serum in PBS/1 % BSA for 1 h. Glass slides were mounted using Superfrost (Matsunami). Fluorescence images were obtained using a fluorescence microscope (Biorevo, KEYENCE).

Biochemical assay of respiratory chain activity

DHODH-dependent and respiratory enzymatic activities were measured by spectrophotometry (U-3210; Hitachi). Stable DHODH-expressing HeLa cells were lysed in a hypotonic buffer (2.5 mM Tris/HCl, pH 7.5, and 2.5 mM $MgCl_2$) on ice for 15 min, and then sonicated for 15 s (25 % output, duty cycle; TAITEC Corp.) to measure respiratory complex activity.

The standard reaction buffer contained 50 mM potassium phosphate, 5 mg/ml BSA and 2.5 mM $MgCl_2$. The substrates (electron donors and electron acceptors) varied depending on the assayed complex. Each reaction was terminated by adding a complex-specific inhibitor. The protein concentration for each reaction was measured by BCA (bicinchoninic acid) protein assay (Thermo). The activities of each complex were indicated by the rate of substrate oxidation or reduction as $nM \cdot min^{-1}$ per mg of protein. Each complex was assayed in the presence of inhibitors of the other complexes to ensure that the activity reflected only the enzyme complex of interest.

DHO–ubiquinone oxidoreductase activity

DHODH activity was determined spectrophotometrically at 37 °C by monitoring the decrease in absorbance at 600 nm of reduced DCPIP (dichlorophenolindophenol; used as an artificial electron acceptor). Briefly, the reaction was initiated with 20 mM DHO in 1 ml of standard reaction buffer supplemented with 50 μM DCPIP, 2 μg of rotenone (a complex I inhibitor), 2 μg of antimycin A (a complex III inhibitor), 5 mM NaN_3 (a complex IV inhibitor) and 0.1 mg of whole cell lysate. The results are expressed as $nmol \cdot min^{-1} \cdot \mu g^{-1}$ of protein. The reaction was stopped by the addition of 2 μg of LFN.

Succinate dehydrogenase (complex II) activity

Succinate dehydrogenase (complex II) activity was determined spectrophotometrically at 37 °C. Briefly, the reaction was initiated with 50 μM DCPIP in 1 ml of standard reaction buffer supplemented with 20 mM succinate, 2 μg of rotenone, 2 μg of antimycin A, 5 mM NaN_3 and 0.1 mg of whole cell lysate. The results are expressed as $nmol \cdot min^{-1} \cdot \mu g^{-1}$ of protein.

Cytochrome c reductase (complex III) activity

Cytochrome *c* reductase (complex III) activity was evaluated spectrophotometrically at 37 °C by monitoring the increase in absorbance at 550 nm of cytochrome *c*. Briefly, the reaction was initiated by the addition of 5 mM decylubiquinone to 1 ml of standard reaction buffer supplemented with 2 μg of rotenone, 5 mM NaN, 60 μM cytochrome *c* and 0.1 mg of whole cell lysate. The reaction was stopped by the addition of 2 μg of antimycin A. The results are expressed as $nmol \cdot min^{-1} \cdot \mu g^{-1}$ of protein.

DHO:cytochrome c oxidoreductase activity

DHO:cytochrome *c* oxidoreductase activity was evaluated similarly to cytochrome *c* reductase activity. The assay was conducted under conditions similar to those for complex III, but using 20 mM DHO as the donor substrate and stopping the reaction with 2 μg of antimycin A. Each data point was recorded in triplicate on a single measurement day.

Protein stability analysis

Wild-type and mutant DHODH-HA were induced by DOX for 24 h, then the cells were treated with 50 μg/ml CHX (cycloheximide) for 0, 2, 4 and 8 h. Western blotting was performed on total protein using the polyclonal anti-DHODH and anti-HA antibodies. The signal intensity was determined.

Statistical analysis

Statistical comparisons between groups were analysed by the Student's *t* test or where appropriate, the paired *t* test. Significance was determined at $P < 0.05$. For all the data, $*P < 0.05$ and $**P < 0.01$.

RESULTS

Establishment of HeLa cell lines stably expressing DHODH

DHODH is a key player in the pyrimidine *de novo* biosynthesis pathway and is coupled to the mitochondrial respiratory chain [17]. As deduced from DHODH cDNA, DHODH comprises 395 amino acids. We predicted an N-terminal mitochondria targeting sequence with a length of 20 amino acids. First, we produced stable cell lines that expressed recombinant DHODH-HA (DHODH with a C-terminal HA tag) upon induction by DOX. Recombinant DHODH-HA was produced in HeLa cells by approximately 5-fold compared with that in non-induced cells at 24 h after induction by DOX (Figure 1A).

DHODH-HA was stained with anti-HA antibodies after induction (Figure 1B); no staining with anti-HA was observed before induction. The HA staining completely co-localized with mitochondria visualized with MitoTracker Red dye, suggesting that the expressed wild-type DHODH-HA was exclusively localized in mitochondria. We observed the same staining pattern using an anti-DHODH antibody (Figure 1B), suggesting that endogenous

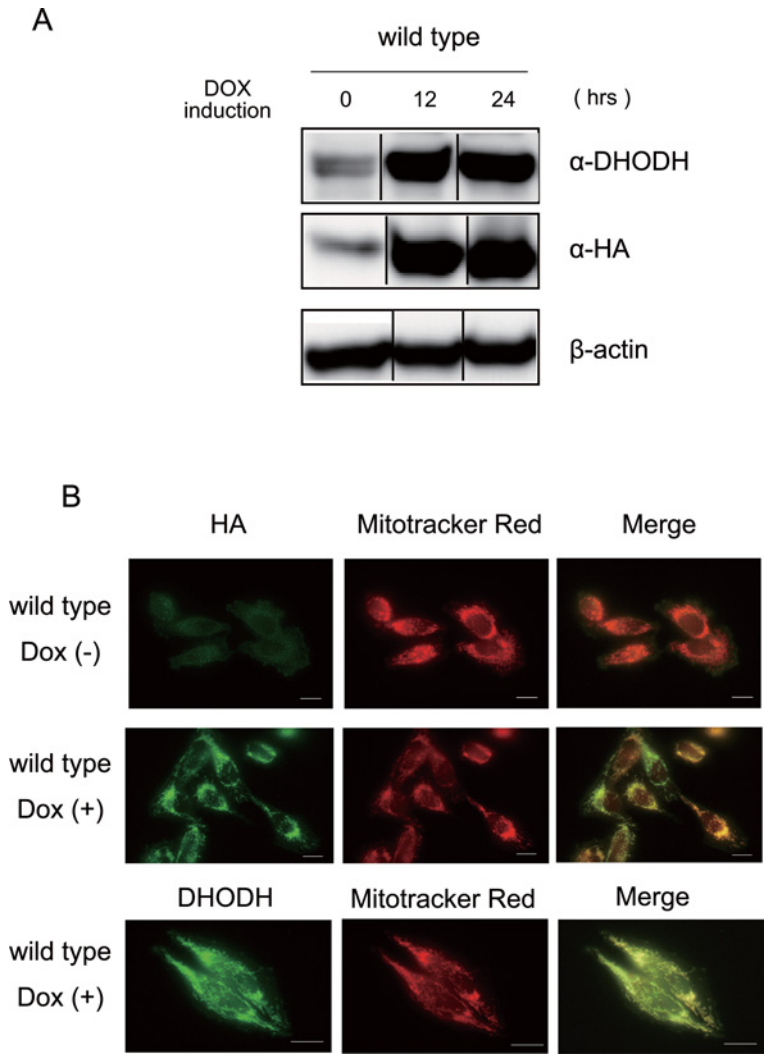

Figure 1 Expression and localization of DHODH-HA protein

(**A**) Inducible expression of recombinant DHODH-HA. DHODH-HA was inducibly expressed in HeLa cells using a Tet-on system. DHODH was detected by immunoblotting with anti-DHODH and anti-HA antibodies. β-Actin was the loading control. Lane 1, no induction; lane 2, 12 h; lane 3, 24 h after DOX treatment. (**B**) Immunocytochemistry of recombinant DHODH. DHODH-HA-transfected cells were cultured in the absence or presence of DOX for 24 h. Mitochondria and recombinant DHODH were visualized with the mitochondria-staining dye MitoTracker Red (centre panels) and anti-HA or anti-DHODH antibodies (left panels) respectively. The right panels show merged images. The scale bars represent 10 μm.

and exogenous DHODH were localized properly in mitochondria.

Expression and localization of DHODH-HA with Miller syndrome-associated mutations

To investigate the effect of Miller syndrome-associated mutations on the processing, localization, and function of DHODH, we introduced three Miller syndrome-associated mutations – G152R, R346W and R135C – into the *DHODH* cDNA (Figure 2A). Arg^{135} is located within the ubiquinone-binding site and the others are located within α-helices.

Next, we produced stable cell lines that expressed recombinant DHODH-HA upon induction by DOX. Recombinant DHODH-HA was produced in HeLa cells by approximately 5-fold compared with that in non-induced cells at 24 h after induction by DOX (Figure 2B). We established HeLa cell lines expressing DOX-induced wild-type or mutant DHODH-HA (Figure 2B).

By immunohistochemistry, R135C-mutant DHODH showed normal subcellular localization with an anti-HA antibody and co-localized with mitochondria in HeLa cells (Figure 2C). The G202A and R346W mutants showed weak staining and co-localization with mitochondria, although the R346W construct also showed weak diffuse staining outside the mitochondria

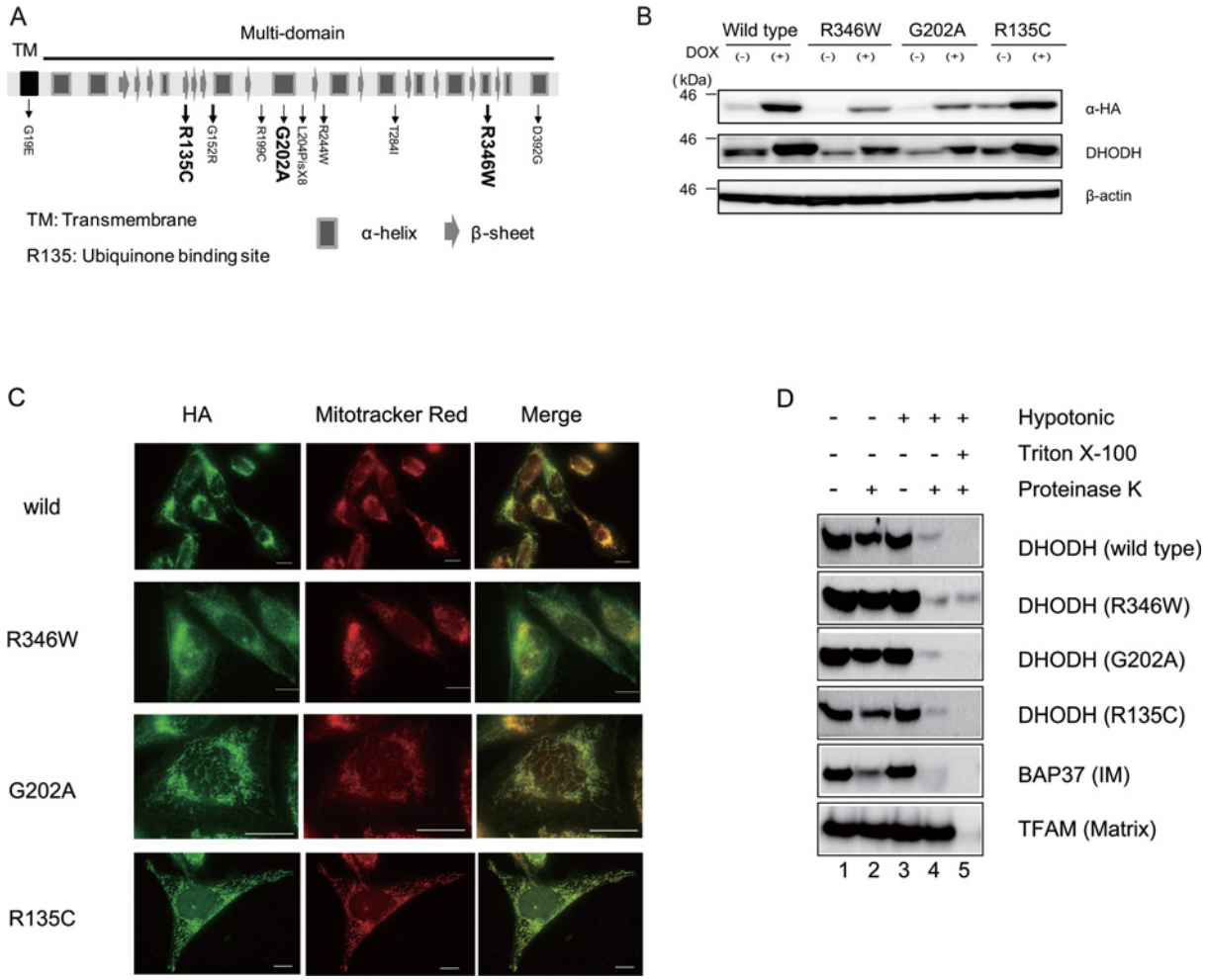

Figure 2 **Expression and localization of Miller syndrome mutations**
(**A**) Schematic representation of the primary structure of DHODH and the location of Miller syndrome-associated mutations. Arg^{135} is the ubiquinone-binding site. TM indicates a transmembrane domain. The 12 α-helices and 13 β-sheet regions are shown as boxes and arrows respectively. We analysed three Miller syndrome mutations R135C, G202A and R346W. (**B**) Inducible expression of wild-type mutant HA-tagged DHODH. Wild-type and mutant HA-tagged DHODH were inducibly expressed in HeLa cells using a Tet-on system. Endogenous and exogenous DHODH were detected by immunoblotting with anti-DHODH and anti-HA antibodies. β-actin was used as the loading control. (**C**) Immunocytochemistry of recombinant mutant DHODH. Mutant DHODH-HA-transfected cells were cultured in the presence of DOX for 24 h. Mitochondria and mutant DHODH were visualized with the mitochondria-staining dye, MitoTracker Red (centre panels) and anti-HA antibodies (left panels) respectively. The right panels show merged images. Scale bar represent 10 μm. (**D**) Submitochondrial localization of exogenous mutant DHODH-HA. Mitochondria were incubated in hypotonic buffer to disrupt the outer membranes without (lanes 3 and 4) or with (lane 5) the non-ionic detergent Triton X-100. Then, the mitochondria were digested with proteinase K (lanes 2, 4 and 5). The indicated proteins were detected by immunoblotting. BAP37 and TFAM are markers of the mitochondrial inner membrane (IM) and matrix respectively.

(Figure 2C). These results suggested that all three mutants were mainly localized in mitochondria; however, a small amount of the R346W mutant protein localized in the cytosol.

Submitochondrial localization of mutant DHODH

Next, we examined the submitochondrial localization of wild-type and mutant DHODH-HA. We disrupted the mitochondrial outer membranes by hypotonic treatment (Figure 2D, lanes 3 and 4 within each group) as verified by the observation that BAP37, which is an inner membrane protein that largely faces the intermembrane space, was digested by proteinase K. On the other hand, TFAM, which localizes in the matrix, was resistant to proteinase K digestion (Figure 2D, lane 4 in the lower panel), indicating that the inner membranes were intact. Under these hypotonic conditions, wild-type and all the mutant DHODH proteins were cleaved by proteinase K (Figure 2D, lane 4). When the inner membranes were solubilized with the non-ionic detergent Triton X-100, both TFAM and DHODH were cleaved by proteinase K (Figure 2D, lane 5). Taken together,

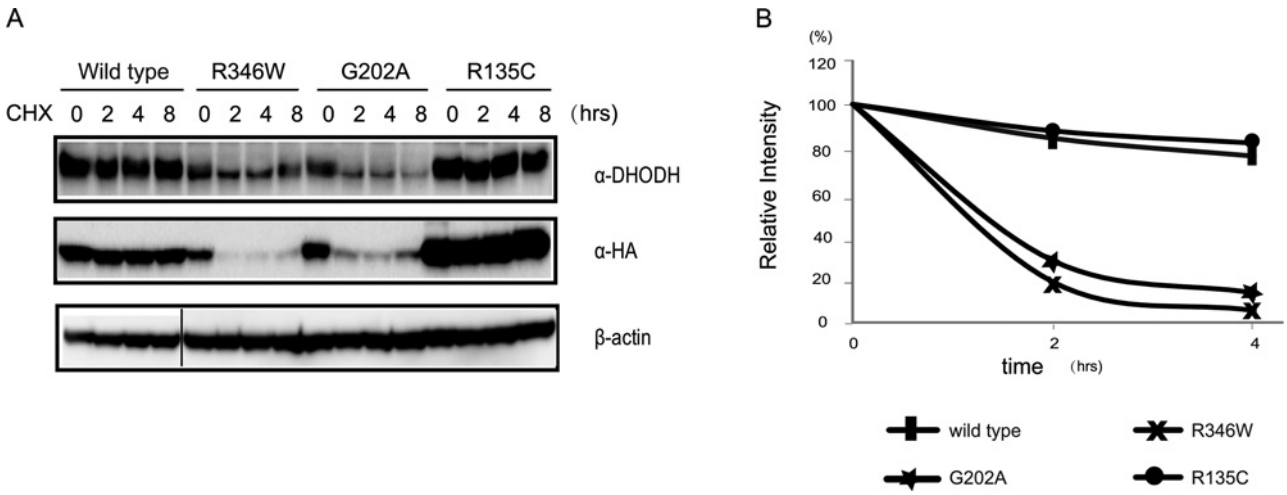

Figure 3 Protein unstability of two mutation of Miller syndrome mutations

(**A**) HeLa cells stably expressing wild-type or mutant DHODH-HA were treated with vehicle (0 h) or 100 μM CHX for 2, 4 or 8 h. Immunoblotting was performed using anti-DHODH and anti-HA antibodies. β-Actin was used as the loading control. (**B**) Relative intensity of α-HA which is shown in (**A**) were plotted after CHX treatment. Treatment of G202A and R346W DHODH-transfected cells with the translation inhibitor CHX significantly decreased the expression levels of mature DHODH protein.

these results suggest that all three mutant DHODH proteins correctly localize in the mitochondrial intermembrane space or inner membrane.

Decreased protein stability of R346W and G202A mutant DHODH

To investigate whether the observed reductions in mutant DHODH protein levels were a consequence of decreased protein stability, we cultured HeLa cells expressing wild-type or mutant DHODH and inhibited new protein translation using CHX after induction by DOX. The amount of the DHODH protein was assessed at 0, 2, 4 and 8 h after CHX treatment. Wild-type and R135C DHODH protein levels remained relatively constant over the 8 h (Figures 3A and 3B). In contrast, R346W and G202A DHODH protein levels were significantly reduced at 2 and 4 h (Figures 3A and 3B), suggesting that the R346W and G202A mutations decreased DHODH protein levels by increasing its rate of degradation. We did not observe destabilization of β-actin (Figure 3A), suggesting that these proteins were specifically degraded by proteasomes or particular protease pathways. As both of these mutations are located within the α-helices of DHODH, they might destabilize the protein structure and accelerate the degradation. The reduction in DHODH protein stability induced by the R346W and G202A mutations may contribute, at least in part, to Miller syndrome.

Wild-type and the R135C mutant showed proper expression of DHODH protein after 24 h induction by DOX. However, the G152R and R346W mutants showed low expression of DHODH-HA after 6 h induction. After 24 h, the *DHODH* mRNA levels were equal for the wild-type and the three mutant constructs (results not shown), suggesting that the G152R and R346W mutant proteins showed reduced protein expression or increased protein turnover.

DHO-dependent ubiquinone and cytochrome *c* oxidoreductase activity in mutant DHODH

As R135C DHODH exhibited no apparent deficiency in stability or intermembrane space sorting, we next examined whether this mutation affected enzymatic function by measuring the DHO-dependent ubiquinone and cytochrome *c* reductase activities. We used wild-type DHODH and two clones of mutant R135C DHODH to measure the enzymatic activities of the respiration complexes. In HeLa cell transfectants, wild-type DHODH showed a 5-fold increase in DHO-dependent enzymatic activity after induction; however, in the R135C mutant, there was no increase in DHO-dependent enzymatic activity after induction of the mutant protein, even if the protein expression increased 5-fold (Figures 1A and 4A). This showed that mutant R135C DHODH had lost its electron-donating function. It has been reported that the Arg^{135} residue is the ubiquinone-binding site in DHODH, suggesting that the R135C mutant would not be able to bind to ubiquinone.

We also compared the respiratory chain activities before and after DOX induction between wild-type and G202A, and R346W mutant DHODH. After DOX induction, the DHO-dependent enzymatic activity of G202A and R346W DHODH increased 2-fold when the protein expression increased to the same extent, suggesting that G202A and R346W DHODH possess functional enzymatic activity but low protein stability (Figure 4B).

Finally, we asked whether the R135C mutant affected the activity of the other respiratory complexes. We compared their

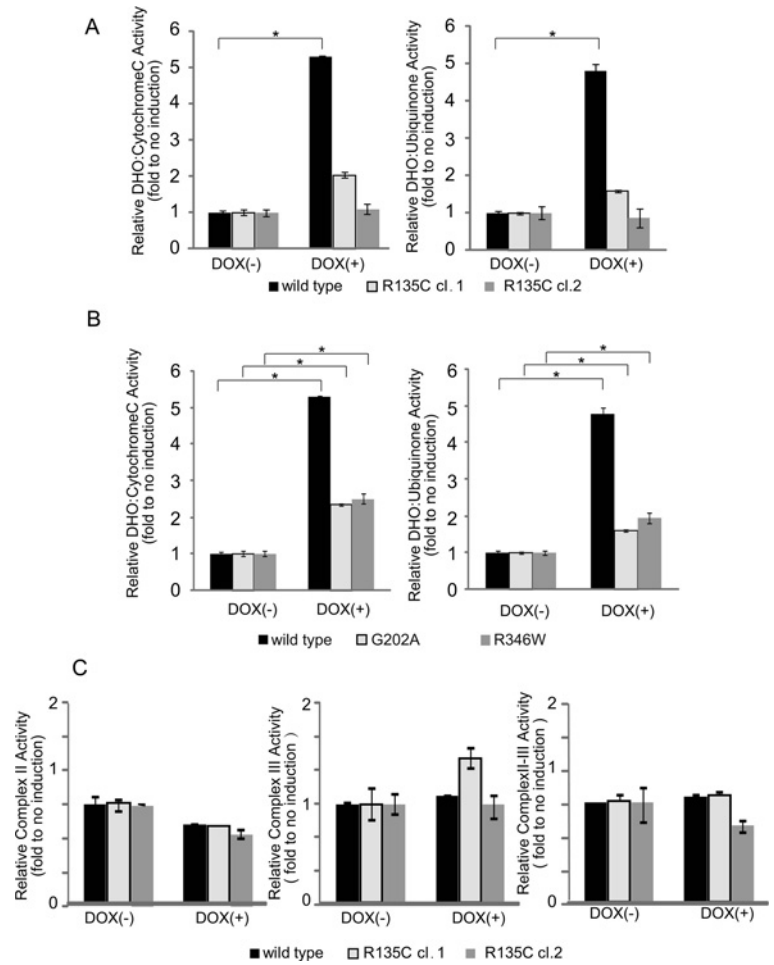

Figure 4 Functional analysis of Miller syndrome mutations

(**A**) Reduced DHO-dependent reductase activities in R135C DHODH-transfected cells. DHO: ubiquinone oxidoreductase activity and DHO: cytochrome *c* oxidoreductase activity were measured using cell lysates as described in the Experimental section. Increased DHO-dependent reductase activity was observed upon the induction of wild-type DHODH; however, induction of R135C DHODH did not result in increased enzymatic activities. The results represent the means $\pm$ S.D. of three independent experiments. $*P<0.05$ compared with controls. (**B**) DHO-dependent reductase activity in G202C and R246W DHODH-expressing cells. DHO: ubiquinone oxidoreductase activity and DHO: cytochrome *c* oxidoreductase activity were measured using cell lysates. A 2-fold increase in DHO-dependent oxidoreductase activity was observed upon the induction of G202A or R346W DHODH. The results represent the means $\pm$ S.D. of three independent experiments. $*P<0.05$ compared with controls. (**C**) The complex II and III activities in R135C and wild-type DHODH were measured using cell lysates as described in the Experimental section. We observed that no difference in the activities of complex II, complex III and the combined complex II–III between R135C and wild-type DHODH.

enzymatic activity after DOX induction. We observed no difference in the activities of complex II, complex III and the combined complex II–III between R135C and wild-type DHODH (Figure 4C). This suggests that R135C DHODH does not directly affect the other respiratory complexes.

DISCUSSION

In the present study, we demonstrated that (i) among Miller syndrome DHODH mutations, G202A and R346W retained proper mitochondrial localization but showed decreased protein stability, (ii) the R135C DHODH mutant showed no DHO-dependent enzymatic activity probably because of structural or functional change of the ubiquinone-binding site at Arg^{135}. We propose that impairment of DHODH activity is linked to the Miller syndrome phenotype.

Miller syndrome is inherited in an autosomal recessive or compound heterozygous pattern [13]. Miller syndrome disrupts the development of the first and second pharyngeal arches. It remains unclear exactly how *DHODH* gene mutations lead to abnormal development of the pharyngeal arches. It is important to note that DHODH is the fourth of six enzymes in the *de novo*

pyrimidine synthesis pathway [8]. The other five enzymes in this pathway constitute two different enzyme complexes located in the cytoplasm. The first three enzymes form the multi-enzyme complex CAD (carbamoyl phosphate synthetase, aspartate transcarbamoylase and dihydro-orotase), and the fifth and sixth enzymes form UMPS.

The *UMPS* gene encodes a bifunctional enzyme with orotate phosphoribosyltransferase and orotidylic decarboxylase activities [18]. Compound heterozygous mutations in the *UMPS* gene cause orotic aciduria, a rare autosomal recessive disorder characterized by megaloblastic anaemia and orotic acid crystalluria that is frequently associated with some degree of physical and mental retardation [19]. However, mutation of *UMPS* does not cause malformation abnormalities as Miller syndrome does, suggesting that, in Miller syndrome, the deficiency of pyrimidine or purine does not cause the craniofacial abnormality.

White et al. [20] reported that the LFN, an inhibitor of DHODH, led to an almost complete abrogation of neural crest development in zebrafish and to a reduction in the self-renewal of mammalian neural crest stem cells. LFN exerts these effects by inhibiting the transcriptional elongation of genes that are required for neural crest development. Particular developmental pathways in neural crest cells have a direct bearing on melanoma formation, suggesting that DHODH is also involved in neural crest cell proliferation and development.

Methotrexate is an inhibitor of *de novo* purine biosynthesis, and its anti-proliferative actions are thought to be due to its inhibition of DHFR (dihydrofolate reductase). The most common pattern of malformation observed in infants with methotrexate-induced embryopathy includes growth deficiency, craniosynostosis, micrognathia and skeletal abnormalities, which are similar to those in individuals with Miller syndrome [21,22]. However, the *DHFR* mutation itself does not result in craniofacial abnormality. Given that Miller syndrome is in part due to some mitochondrial dysfunction, methotrexate might not only target DHFR but also the mitochondria in neural crest cells.

Many birth defects, such as Miller syndrome and methotrexate-induced embryopathy, are associated with craniofacial malformations. These data suggest that the development of neural crest stem cells is involved in craniofacial malformations [23], and that the malformations observed in individuals with Miller syndrome could be caused by failure of correct neural crest cell development because of loss of DHODH function.

Human DHODH is composed of two domains, a large C-terminal domain (residues 78–396) and a smaller N-terminal domain (residues 30–68), connected by an extended loop. The large C-terminal domain can be best described as an α/β-barrel fold with a central barrel of eight parallel β-strands surrounded by eight α helices. There are some proximal redox sites and the domain ends with several charged or polar side chains (Gln^{47}, Tyr^{356}, Thr^{360} and Arg^{135}). Arg^{135}, which is located at the ubiquinone-binding site, is conserved from humans to *Plasmodium falciparum*. We observed that R135C-mutated DHODH, which has been reported in Miller syndrome, showed proper mitochondrial localization but no DHO-dependent enzymatic activity. Because the α- and β-barrel domains of DHODH form a tunnel to the active site of enzymatic activity, compounds interacting with the α- and the β-barrel domains can block DHODH activity. G202A and R346W are located in the α-barrel domains of DHODH; the G202R and R346W mutations would be expected to result in conformational changes that lead to unstable proteins.

In these experiments, we observed, for the first time, that the G202A and R346W mutations cause deficient protein stability, and R135C mutation impairs the substrate-induced enzymatic activity, suggesting that impairment of DHODH activity is linked to the Miller syndrome phenotype.

AUTHOR CONTRIBUTION

JingXian Fang designed experiments, conducted experiments, analysed data and wrote the paper; Takeshi Uchiumi designed experiments, analysed data and wrote the paper; Mikako Yagi, Shinya Matsumoto, Toshirou Saitoh, Shinya Takazaki and Rie Amamoto conducted experiments and analysed data; Tomotake Kanki, Haruyoshi Yamaza and Kazuaki Nonaka designed experiments, analysed data and wrote the paper; and Dongchon Kang designed experiments and wrote the paper.

ACKNOWLEDGEMENTS

We acknowledge the technical expertise of the staff of the Support Center for Education and Research, Kyushu University.

FUNDING

This work was supported in part by Grants-in-Aid for Scientific Research from the Ministry of Education, Culture, Sports, Science and Technology of Japan [grant numbers 24590387 and 22249018].

REFERENCES

1 McBride, H. M., Neuspiel, M. and Wasiak, S. (2006) Mitochondria: more than just a powerhouse. Curr. Biol. **16**, R551–R560
2 DiMauro, S. and Schon, E. A. (2008) Mitochondrial disorders in the nervous system. Annu. Rev. Neurosci. **31**, 91–123
3 Frenzel, M., Rommelspacher, H., Sugawa, M. D. and Dencher, N. A. (2010) Ageing alters the supramolecular architecture of OxPhos complexes in rat brain cortex. Exp. Gerontol. **45**, 563–572
4 Wallace, D. C. (2010) Mitochondrial DNA mutations in disease and aging. Environ. Mol. Mutagen. **51**, 440–450
5 Tuppen, H. A., Blakely, E. L., Turnbull, D. M. and Taylor, R. W. (2010) Mitochondrial DNA mutations and human disease. Biochim. Biophys. Acta **1797**, 113–128
6 Loffler, M., Grein, K., Knecht, W., Klein, A. and Bergjohann, U. (1998) Dihydroorotate dehydrogenase. Profile of a novel target for antiproliferative and immunosuppressive drugs. Adv. Exp. Med. Biol. **431**, 507–513
7 Evans, D. R. and Guy, H. I. (2004) Mammalian pyrimidine biosynthesis: fresh insights into an ancient pathway. J. Biol. Chem. **279**, 33035–33038

8 Rawls, J., Knecht, W., Diekert, K., Lill, R. and Loffler, M. (2000) Requirements for the mitochondrial import and localization of dihydroorotate dehydrogenase. Eur. J. Biochem. **267**, 2079–2087
9 Loffler, M., Jockel, J., Schuster, G. and Becker, C. (1997) Dihydroorotate-ubiquinone oxidoreductase links mitochondria in the biosynthesis of pyrimidine nucleotides. Mol. Cell. Biochem. **174**, 125–129
10 Walse, B., Dufe, V. T., Svensson, B., Fritzson, I., Dahlberg, L., Khairoullina, A., Wellmar, U. and Al-Karadaghi, S. (2008) The structures of human dihydroorotate dehydrogenase with and without inhibitor reveal conformational flexibility in the inhibitor and substrate binding sites. Biochemistry **47**, 8929–8936
11 Miller, M., Fineman, R. and Smith, D. W. (1979) Postaxial acrofacial dysostosis syndrome. J. Pediatr. **95**, 970–975
12 Donnai, D., Hughes, H. E. and Winter, R. M. (1987) Postaxial acrofacial dysostosis (Miller) syndrome. J. Med. Genet. **24**, 422–425
13 Ng, S. B., Bigham, A. W., Buckingham, K. J., Hannibal, M. C., McMillin, M. J., Gildersleeve, H. I., Beck, A. E., Tabor, H. K., Cooper, G. M., Mefford, H. C. et al. (2010) Exome sequencing identifies MLL2 mutations as a cause of Kabuki syndrome. Nat. Genet. **42**, 790–793
14 Kinoshita, F., Kondoh, T., Komori, K., Matsui, T., Harada, N., Yanai, A., Fukuda, M., Morifuji, K. and Matsumoto, T. (2011) Miller syndrome with novel dihydroorotate dehydrogenase gene mutations. Pediatr. Int. **53**, 587–591
15 Fukushima, R., Kanamori, S., Hirashiba, M., Hishikawa, A., Muranaka, R. I., Kaneto, M., Nakamura, K. and Kato, I. (2007) Teratogenicity study of the dihydroorotate–dehydrogenase inhibitor and protein tyrosine kinase inhibitor Leflunomide in mice. Reprod. Toxicol. **24**, 310–316
16 Uchiumi, T., Ohgaki, K., Yagi, M., Aoki, Y., Sakai, A., Matsumoto, S. and Kang, D. (2010) ERAL1 is associated with mitochondrial ribosome and elimination of ERAL1 leads to mitochondrial dysfunction and growth retardation. Nucleic Acids Res. **38**, 5554–5568
17 Ruckemann, K., Fairbanks, L. D., Carrey, E. A., Hawrylowicz, C. M., Richards, D. F., Kirschbaum, B. and Simmonds, H. A. (1998) Leflunomide inhibits pyrimidine *de novo* synthesis in mitogen-stimulated T-lymphocytes from healthy humans. J. Biol. Chem. **273**, 21682–21691
18 McClard, R. W., Black, M. J., Livingstone, L. R. and Jones, M. E. (1980) Isolation and initial characterization of the single polypeptide that synthesizes uridine 5′-monophosphate from orotate in Ehrlich ascites carcinoma. Purification by tandem affinity chromatography of uridine-5′-monophosphate synthase. Biochemistry **19**, 4699–4706
19 Suchi, M., Mizuno, H., Kawai, Y., Tsuboi, T., Sumi, S., Okajima, K., Hodgson, M. E., Ogawa, H. and Wada, Y. (1997) Molecular cloning of the human UMP synthase gene and characterization of point mutations in two hereditary orotic aciduria families. Am. J. Hum. Genet. **60**, 525–539
20 White, R. M., Cech, J., Ratanasirintrawoot, S., Lin, C. Y., Rahl, P. B., Burke, C. J., Langdon, E., Tomlinson, M. L., Mosher, J., Kaufman, C. et al. (2011) DHODH modulates transcriptional elongation in the neural crest and melanoma. Nature **471**, 518–522
21 Milunsky, A., Graef, J. W. and Gaynor, Jr, M. F. (1968) Methotrexate-induced congenital malformations. J. Pediatr. **72**, 790–795
22 Wheeler, M., O'Meara, P. and Stanford, M. (2002) Fetal methotrexate and misoprostol exposure: the past revisited. Teratology **66**, 73–76
23 Minoux, M. and Rijli, F. M. (2010) Molecular mechanisms of cranial neural crest cell migration and patterning in craniofacial development. Development **137**, 2605–2621

Received 14 May 2012/31 July 2012; accepted 1 August 2012
Published as Immediate Publication 11 September 2012, doi 10.1042/BSR20120046